

Mathematical modeling of zebrafish social behavior in response to acute caffeine administration

Mohammad Tuqan¹, and Maurizio Porfiri^{1,2,3,*}

¹ Department of Mechanical and Aerospace Engineering
New York University, Tandon School of Engineering, New York, USA

² Center for Urban Science + Progress
New York University, New York, USA

³ Department of Biomedical Engineering
New York University, Tandon School of Engineering, New York, USA

Correspondence*:
Maurizio Porfiri
mporfiri@nyu.edu

2 ABSTRACT

3 Zebrafish is a model organism that is receiving considerable attention in preclinical research.
4 Particularly important is the use of zebrafish in behavioral pharmacology, where a number of high-
5 throughput experimental paradigms have been proposed to quantify the effect of psychoactive
6 substances consequences on individual and social behavior. In an effort to assist experimental
7 research and improve animal welfare, we propose a mathematical model for the social behavior
8 of groups of zebrafish swimming in a shallow water tank in response to the administration of
9 psychoactive compounds to select individuals. We specialize the mathematical model to caffeine,
10 a popular anxiogenic compound. Each fish is assigned to a Markov chain that describes transitions
11 between freezing and swimming. When swimming, zebrafish locomotion is modeled as a pair of
12 coupled stochastic differential equations, describing the time evolution of the turn-rate and speed
13 in response to caffeine administration. Comparison with experimental results demonstrate the
14 accuracy of the model and its potential use in the design of *in-silico* experiments.

15 **Keywords:** Anxiety, collective behavior, *Danio rerio*, *in-silico*, pharmacology, social interaction, stochastic differential equations

16 **Word count:** 6897

1 INTRODUCTION

17 Animal experiments are a standard practice for hypothesis testing in preclinical research (Chow et al.,
18 2008; Sánchez Morgado and Brønstad, 2021). However, experimental studies involving pharmacological
19 treatment of sentient animals continue to raise ethical concerns regarding the well-being of the animals
20 (Badyal and Desai, 2014). Computational methods can enable *in-silico* experiments that might help in
21 the fulfillment of the 3Rs: Reducing the number of subjects, Refining experimental design and setup, and
22 Replacing the use of live subjects (Ford, 2016; Raunio, 2011; Viceconti et al., 2021).

23 Zebrafish (*Danio rerio*) has emerged as a species of choice in experimental studies in pharmacology where
24 it is used in high throughput drug screening of several psychoactive compounds (Goldsmith, 2004; Guo,

25 2004). Its genetic and physiologic similarities with humans have made the zebrafish an attractive species for
26 experimental investigations of human dysfunctional processes (Stewart et al., 2014). In particular, zebrafish
27 experiments could clarify some of the open questions on anxiety-related behaviors in human (Stewart et al.,
28 2012). In these experiments, fish behavior is monitored in an experimental setup to investigate how anxiety-
29 related behavior is modulated by anxiolytic and anxiogenic compounds, such as caffeine, cocaine, and
30 ethanol (da Silva Chaves et al., 2018; Egan et al., 2009; Gerlai et al., 2008; Kacprzak et al., 2017; Speedie
31 and Gerlai, 2008). Experiments on fish treated with such compounds have revealed numerous anxiety-
32 related behaviors; erratic activity (jump turns and sudden change in direction), thigmotaxis (tendency to
33 stay near the wall), geotaxis (tendency to stay at the bottom of the tank), and freezing (Cachat et al., 2010;
34 Khan et al., 2017; Maximino et al., 2010a).

35 Previous efforts have leveraged data-driven, mathematical models to accurately describe the locomotion
36 of isolated fish swimming in shallow or deep water tanks (Burbano-Lombana and Porfiri, 2020; Gautrais
37 et al., 2009; Mwaffo and Porfiri, 2015; Mwaffo et al., 2017a; Zienkiewicz et al., 2015). With respect to
38 zebrafish, a number of efforts have sought to incorporate their unique burst-and-coast swimming style,
39 composed of sudden tail bursts that are followed by coasting phases (Blake, 2004; Chung, 2009). The
40 general line of approach consists of formulating a stochastic differential equation (SDE) for the turn-rate
41 evolution, in which white noise is superimposed to intermittent excitation in the form of a jump process
42 (Mwaffo et al., 2015). The original jump persistent turning walker (JPTW) was later adapted to the study
43 of the effect of psychoactive manipulations in two separate studies (Burbano-Lombana and Porfiri, 2020;
44 Mwaffo and Porfiri, 2015). Mwaffo and Porfiri (2015) investigated the effect of acute ethanol treatment of
45 zebrafish on model parameters of the JPTW, discovering a strong effect of concentration on the parameters
46 of the jump process. Burbano-Lombana and Porfiri (2020) expanded on JPTW to simulate zebrafish
47 response to acute caffeine administration. Not only did the model account for speed modulation during
48 locomotion through an additional SDE, but also did it incorporate a detailed treatment of freezing episodes
49 using discrete-time Markov chain. Overall, these studies provide indication of the sensitivity of model
50 parameters to the administration of psychoactive compounds that must be considered when performing
51 projective, *in-silico* experiments.

52 Other studies have extended individual fish models to groups, thereby including fish social interactions in
53 terms of schooling and shoaling behaviors. In these models, social interaction is introduced as a response
54 function that modulates the speed and turn-rate. Visual stimuli associated with the presence of conspecifics
55 have been often considered in these models (Butail et al., 2016; Calovi et al., 2015, 2018; Collignon et al.,
56 2016; Gautrais et al., 2012; Mwaffo et al., 2017b; Zienkiewicz et al., 2015, 2018), where fish tend to
57 align and swim closer to neighboring subjects accommodating to alignment and attraction forces. Related
58 efforts have included hydrodynamic interactions to incorporate lateral line sensing of the flow caused by
59 neighboring subjects (Filella et al., 2018; Gazzola et al., 2016; Jhawar et al., 2020; Porfiri et al., to appear).
60 Overall, the mathematical underpinnings of these studies are common to the investigation of the structure
61 of collective behavior of several species, from ants (Valentini et al., 2020) to bats (Shirazi and Abaid, 2018).

62 To the best of our knowledge, models looking at the effect of psychoactive compounds on zebrafish
63 social behavior have never been explained in the literature. Here, we fill this gap by proposing a model
64 that not only captures the effect of caffeine administration on fish locomotory activity but also takes
65 into consideration the influence of the social environment in modulating the pharmacological response.
66 To this end, we model fish dynamics in terms of speed and turn-rate, along two time-scales similar to
67 Burbano-Lombana and Porfiri (2020). We define a slow time-scale that captures the transitions between
68 swimming and freezing states using a discrete-time Markov chain. During the swimming state, we model

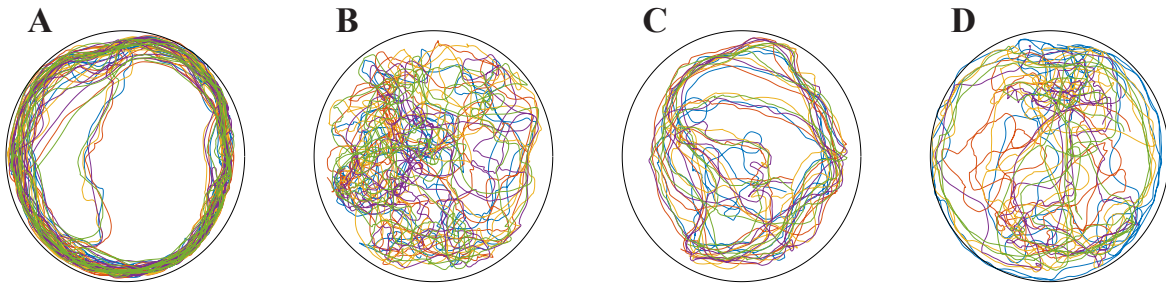


Figure 1. Representative trajectories of a group of five subjects, with four untreated individuals and one subjects treated at a caffeine concentration of: 0 (**A**), 25 (**B**), 50 (**C**), and 70 mg/L (**D**).

69 the speed and turn-rate evolution along a fast time-scale as a system of coupled SDEs. In the evolution of
 70 the turn-rate, we account for social interactions for each subject based on visual cues from neighboring
 71 individuals, therein, we utilize different interaction parameters depending on the treatment of the specific
 72 subject. To calibrate the model parameters, we rely on the experimental data-set from Neri et al. (2019),
 73 wherein a group of untreated subjects swam with a caffeine-treated individual. For each experimental
 74 trial, we estimate the transition probabilities of the Markov chain by counting the instances of freezing
 75 and swimming for each fish within the group. Further, we calibrate the locomotion and social interaction
 76 parameters of the governing SDEs for each fish in the group using maximum likelihood estimation.

77 We investigate the value of the social group in modulating the response of fish to caffeine administration.
 78 Specifically, we compare calibrated model parameters for a treated fish swimming with an untreated group
 79 with those of a treated fish swimming in isolation from Burbano-Lombana and Porfiri (2020). We further
 80 highlight an asymmetric interaction between the treated individual and untreated subjects, associated with
 81 the effect of caffeine on locomotory activity of fish and how it is perceived by untreated subjects (Gupta
 82 et al., 2014; Miller and Gerlai, 2007; Speedie and Gerlai, 2008). Lastly, we verify the predictive ability of
 83 the proposed model in capturing the social behavior of the group by comparing a set of social interaction
 84 metrics obtained from *in-silico* experiments to those from real experiments.

85 We structure the rest of the paper as follows. We start with a synoptic description of the experiments and
 86 data in Section 2. In Section 3, we present our modeling framework and define the speed and turn-rate
 87 evolution models. Additionally, we describe the model discretization and calibration approach. In Section
 88 4, we discuss the influence of caffeine concentration on individual and social parameters of the treated fish
 89 and validate the proposed model through comparisons with experimental data. We conclude in Section 5
 90 with a discussion on the general findings of this work and possible research directions for future work.

2 MATERIALS AND EQUIPMENT

91 Our theoretical endeavor is grounded in experiments from Neri et al. (2019) (approved by the Animal
 92 Welfare Committee of New York University: protocol number 13–1424) on the effect of acute caffeine
 93 treatment on social behavior. Below, we summarize the main components of the experimental framework
 94 and data analysis from Neri et al. (2019).

95 2.1 Experiment setup and procedure

96 The setup consisted of a circular tank of diameter $d = 90$ cm filled with water at depth $h = 10$ cm.
 97 Cameras were used to record fish behavior at 40 frames/s for a duration of five minutes ($T_{\text{exp}} = 300$ s).

98 Videos were processed by an in-house multitarget tracking system developed in MATLAB (Ladu et al.,
99 2014).

100 Experiments were performed on groups of five adult subjects, including four untreated individuals and
101 one treated individual, at four different caffeine concentrations: 0 (vehicle), 25, 50, and 70 mg/L. For each
102 trial, five fish were randomly chosen from the holding tank. 50 fish were chosen at random to conduct ten
103 experimental trials for each caffeine concentration (200 fish in total). One of the fish was kept in a 0.5 L
104 beaker of a caffeine solution for one hour. Four untreated fish were introduced to the circular arena at the
105 same time the beaker with the treated fish was placed in the arena. After ten minutes of habituation, the
106 treated fish was hand-netted from the beaker and released into the arena. The average fish body length (BL)
107 was approximately 3 cm.

108 2.2 Data post-processing

109 Fish trajectories were obtained by tracking the centroid of each fish. Figure 1 illustrates representative
110 trajectories from each concentration. The trajectory of the i -th fish is denoted by $(x_i(k\Delta), y_i(k\Delta))$, where
111 $\Delta = 0.025$ s is the sampling time, and $k \in [1, \dots, K = \frac{T_{\text{exp}}}{\Delta}]$.

112 Position increments between consecutive readings were used to obtain the velocity $\mathbf{v}_i(k\Delta) =$
113 $[v_{i,x}(k\Delta), v_{i,y}(k\Delta)]^T$ and the speed $v_i(k\Delta) = \sqrt{v_{i,x}^2(k\Delta) + v_{i,y}^2(k\Delta)}$. To calculate the turn-rate, $\omega_i(k\Delta)$,
114 we estimated the fish heading, $\theta_i(k\Delta)$, by fitting three consecutive positions, $(x_i((k-1)\Delta), y_i((k-1)\Delta))$,
115 $(x_i(k\Delta), y_i(k\Delta))$, and $(x_i((k+1)\Delta), y_i((k+1)\Delta))$, along a circle (Gautrais et al., 2009). The turn-rate
116 was then inferred from the heading increment, $\delta\theta_i(k\Delta)$, between the two lines connecting the center of the
117 circle with the $(k-1)$ -th and $(k+1)$ -th centroid position on the circle as $\omega_i(k\Delta) = \frac{\delta\theta_i(k\Delta)}{2\Delta}$. Without loss
118 of generality, we take $i = 1$ as the treated fish throughout this paper.

119 Fish trajectories were also used to score the time spent freezing, an anxiety-related behavior in zebrafish
120 (Maximino et al., 2010a). Following Kopman et al. (2013), a fish was considered to be in a freezing episode
121 if it stayed within 2 cm radius for at least $T_F = 2$ s. From experimental data, we defined a binary Boolean
122 variable $\Gamma_i(nT_F)$, with $n = [1, \dots, \frac{T_{\text{exp}}}{T_F}]$ that recorded instances of swimming ($\Gamma_i(nT_F) = 1$) and freezing
123 ($\Gamma_i(nT_F) = 0$).

124 Four experimental trials were discarded due to recording issues (two from 0 mg/L, and two from
125 50 mg/L). We omitted four additional experimental trials due to insufficient data points for experimental
126 analysis and parameter calibration (two from 25 mg/L, and two from 70 mg/L), whereby the fish spent
127 less than 10 s in the swimming state and more than two BL away from the wall. For this reason, the
128 experimental results presented in this paper may differ from that presented in Neri et al. (2019) that relies
129 on the same data-set.

3 METHODS

130 Here, we introduce the proposed data-driven framework to study the effect of caffeine treatment on
131 individual and social behavior. With respect to our previous work (Burbano-Lombana and Porfiri, 2020),
132 this study contributes a detailed model of social behavior, including attraction and alignment between
133 subjects. Most importantly, these parameters are functions of the caffeine concentration and vary between
134 treated and untreated subjects.

135 With respect to the state of the art on social behavior, the proposed model brings forward the critical role
136 of the freezing response, by developing a two-time-scale modeling dichotomy where freezing evolves a
137 slow time-scale that dictates when the animal is swimming or motionless. During locomotion, we use two

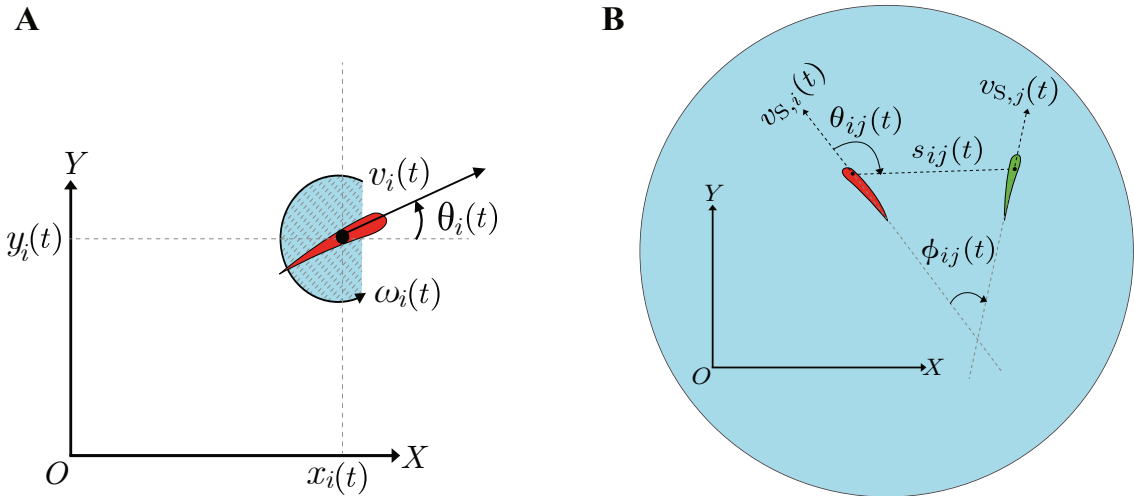


Figure 2. (A) Fish kinematics: at time t , the fish pose is denoted as $[x_i(t), y_i(t), \theta_i(t)]^T$, swimming at speed $v_i(t)$ and turn-rate $\omega_i(t)$. (B) A close-up look at the interaction between a pair of fish within a group of five fish. Alignment and attraction between the i - and j -th fish are functions of the relative orientation, $\phi_{ij}(t)$, and relative position, in terms of the distance between fish, $s_{ij}(t)$, and relative angle, $\theta_{ij}(t)$.

138 coupled stochastic differential equations (SDEs) to describe the evolution of the turn-rate and the speed.
 139 The variables and notation used in the manuscript are included in Tab. S1 in the supplemental material.

140 3.1 Zebrafish kinematics

141 The fish were swimming in a shallow water tank, such that we could consider a two-dimensional (2D)
 142 model to describe their motion. Each fish is modeled as a rigid body, moving in a global reference frame
 143 $[X, Y]$ with origin O . The position of the centroid of fish i at time t is denoted as $[x_i(t), y_i(t)]^T$. We also
 144 measure the heading $\theta_i(t) \in [-\pi, \pi]$ as the angle between the swimming velocity and the global reference
 145 frame. Hence, the pose of fish i is described as a three-dimensional vector $[x_i(t), y_i(t), \theta_i(t)]^T$, as shown in
 146 Fig. 2A. The evolution of zebrafish pose is modeled as a first-order kinematic model

$$\begin{bmatrix} \dot{x}_i(t) \\ \dot{y}_i(t) \\ \dot{\theta}_i(t) \end{bmatrix} = \begin{bmatrix} v_i(t) \cos \theta_i(t) \\ v_i(t) \sin \theta_i(t) \\ \omega_i(t) \end{bmatrix}, \quad (1)$$

147 with initial conditions $x_i(0) = x_{0,i}$, $y_i(0) = y_{0,i}$, and $\theta_i(0) = \theta_{0,i}$. Here, $v_i(t)$ and $\omega_i(t)$ are the speed and
 148 turn-rate of the fish, respectively. We develop a mathematical model for the time-evolution of $v_i(t)$ and
 149 $\omega_i(t)$ to predict the individual and social response of zebrafish.

150 3.2 Zebrafish dynamics

151 3.2.1 Freezing model

152 We adopt a discrete-time Markov chain to capture the transitions between freezing and swimming
 153 states. Building on the work of Burbano-Lombana and Porfiri (2020) on isolated animals, for the i -th
 154 fish, we introduce a binary process $\Gamma_i(nT_F)$ that takes values 0 (freezing, F) and 1 (swimming, S), where
 155 $n = [1, \dots, \Upsilon]$, $\Upsilon = \frac{T_{\text{sim}}}{T_F}$, and T_{sim} is the total simulation time. The Markov chain is determined by
 156 probabilities of persistence in swimming and freezing states, $p_{S,i}$ and $p_{F,i}$, respectively, and probabilities
 157 of state transition, given by $p_{SF,i} = 1 - p_{S,i}$ and $p_{FS,i} = 1 - p_{F,i}$, respectively.

158 The speed and turn-rate of the i -th fish are

$$v_i(t) = \begin{cases} 0, & \text{if } \Gamma_i(nT_F) = 0 \\ v_{S,i}(t), & \text{if } \Gamma_i(nT_F) = 1 \end{cases}, \quad (2a)$$

$$\omega_i(t) = \begin{cases} 0, & \text{if } \Gamma_i(nT_F) = 0 \\ \omega_{S,i}(t), & \text{if } \Gamma_i(nT_F) = 1 \end{cases}, \quad (2b)$$

159 such that during a freezing episode both the speed and turn-rate are zero and during swimming they evolve
160 on the basis of the SDEs described below.

161 3.2.2 Locomotion and interaction models

162 Speed and turn-rate in the swimming state are modeled as a system of two coupled SDEs. In the model, we
163 include social interaction terms that modulate fish locomotion based on the visual cues from neighboring
164 conspecifics. As illustrated in Fig. 2B, we describe fish schooling between the focal fish, i , and the
165 neighboring fish, j , in terms of the relative orientation, $\phi_{ij}(t) = \theta_i(t) - \theta_j(t)$. Further, we examine fish
166 shoaling in terms of the relative position of the neighboring fish with respect to the focal fish expressed in
167 terms of the distance between the pair of fish, $s_{ij}(t)$, and relative angle, $\theta_{ij}(t)$.

168 To model the evolution of the speed, we adopt the following logistic model, similar to Burbano-Lombana
169 and Porfiri (2020) for a single fish (Pasquali, 2001):

$$dv_{S,i}(t) = (\eta_i v_{S,i}(t) - g(\omega_{S,i}(t))v_{S,i}^2(t)) dt + \sigma_{v,i} v_{S,i}(t) dW_{v,i}(t), \quad (3)$$

170 where η_i [s^{-1}] and $\sigma_{v,i}$ [$s^{-\frac{1}{2}}$] are the linear expansion rate and the strength of the added noise, respectively;
171 $W_{v,i}(t)$ is a standard Wiener process; and $g(\omega_{S,i}(t))$ [m^{-1}] encapsulates the effect of the turn-rate.
172 Specifically, the speed response function is

$$g(\omega_{S,i}(t)) = \frac{1}{\text{std}_{\omega,i} \text{BL}} |\omega_{S,i}(t)|, \quad (4)$$

173 where $\text{std}_{\omega,i}$ is the standard deviation of the absolute instantaneous value of the turn-rate (Burbano-
174 Lombana and Porfiri, 2020). This function captures the need of fish to slow down when turning, while
175 attaining larger speeds during straight swimming.

176 This model offers a first approximation of speed modulation during social behavior. For each fish, the
177 model requires the calibration of two parameters, assuming that the body length is common to the entire
178 group: η_i , and $\sigma_{v,i}$. In this basic incarnation, the model does not incorporate speed-based social interaction,
179 which have been proposed by several authors to play some role in the social response of social fish (Berdahl
180 et al., 2013; Herbert-Read et al., 2011, 2013; Katz et al., 2011; Krause et al., 2005). The choice of neglecting
181 social interactions mediated by the speed is due to the need of reducing the number of model parameters,
182 magnified by the presence of individual differences in the treatment of the group.

183 The turn-rate dynamics are captured by the JPTW (Mwaffo et al., 2015; Zienkiewicz et al., 2018),

$$d\omega_{S,i}(t) = -\alpha_i(\omega_{S,i}(t) - \omega_{S,i}^*(t)) + f_w(\phi_{w,i}(t), d_{w,i}(t))dt + \sigma_{\omega,i}dW_{\omega,i}(t) + dJ_i(t), \quad (5)$$

184 where $\omega_{S,i}^*(t)$ [rad s^{-1}] is the turn-rate interaction response function; $f_w(\phi_{w,i}(t), d_{w,i}(t))$ is the wall
 185 interaction function where $\phi_{w,i}(t)$ is the projected angle to collision and $d_{w,i}(t)$ is the distance from the
 186 wall; α_i [s^{-1}] is a positive parameter quantifying the relaxation rate; $\sigma_{\omega,i}$ [$\text{rad s}^{-\frac{3}{2}}$] is the strength of the
 187 added noise; $W_{\omega,i}(t)$ is a standard Wiener process; and $J_i(t)$ is the jump noise term encapsulating sudden
 188 changes in the turn-rate.

189 Due to the presence of the caffeine treatment, the social interaction gains will vary in the group. Not only
 190 do we expect untreated fish to respond differently to a treated fish compared to untreated fish, but also
 191 we anticipate the interaction between treated and untreated subjects to be asymmetric. These claims are
 192 grounded in two propositions from the literature. First, the anxiogenic value of caffeine has been shown
 193 to influence the tendency of the caffeine-treated fish to interact with untreated conspecifics (Miller and
 194 Gerlai, 2007; Speedie and Gerlai, 2008). Second, the psychostimulatory nature of caffeine is known to
 195 influence the locomotory response of the animals (Gupta et al., 2014), which may underlie differences in
 196 the appraisal of treated fish by untreated individuals. Accordingly, the turn-rate response function is written
 197 as

$$\omega_{S,i}^*(t) = \sum_{j=1}^N \Gamma_j(nT_F)[k_{p,ij} s_{ij}(t) \sin \theta_{ij}(t) + k_{v,ij} v_{S,i}(t) \sin \phi_{ij}(t)], \quad (6)$$

198 where $k_{p,ij}$ [$\text{rad m}^{-1} \text{s}^{-1}$] and $k_{v,ij}$ [rad m^{-1}] are the attraction and alignment gains of fish i toward fish
 199 j , respectively. For each trial, the model requires calibrating $2N - 1$ pairs of gains. We categorize these
 200 parameters based on the direction of interaction as follows:

$$k_{p,ij} = \begin{cases} k_{p_{\text{TU}}}, & \text{if } i = 1, j \neq i \\ k_{p_{\text{UT},i}}, & \text{if } i \neq 1, j = 1 \\ k_{p_{\text{UU},i}}, & \text{if } i \neq 1, j \neq 1 \end{cases} \quad (7a)$$

$$k_{v,ij} = \begin{cases} k_{v_{\text{TU}}}, & \text{if } i = 1, j \neq i \\ k_{v_{\text{UT},i}}, & \text{if } i \neq 1, j = 1 \\ k_{v_{\text{UU},i}}, & \text{if } i \neq 1, j \neq 1 \end{cases} \quad (7b)$$

201 where TU, UT, and UU identify the response of the treated to untreated fish, the untreated to the treated
 202 fish, and the interaction between untreated subjects, respectively. The presence of $\Gamma_j(nT_F)$ in Eq. (6) is
 203 used to selectively limit the social response of fish to the group members that are actively swimming. Fish
 204 that are freezing are excluded from the social interaction model, based on calibration of the model on real
 205 data as well as biological observations that suggest zebrafish are more responsive to dynamic, rather than
 206 static stimuli (Ruberto et al., 2016).

207 The wall interaction function is written as follows (Burbano-Lombana and Porfiri, 2020; Gautrais et al.,
 208 2009):

$$f_w(\phi_{w,i}(t), d_{w,i}(t)) = a_w \text{sgn}(\phi_{w,i}(t)) e^{-d_{w,i}(t)b_w}, \quad (8)$$

209 where the intensity of wall interactions, a_w [rad s^{-1}], and the sensitivity of the fish to visual stimulus to
 210 the wall, b_w [cm^{-1}], are two positive parameters. We hypothesize that all fish interact in the same way
 211 with the environment, such that the two parameters a_w and b_w are the same for the entire group and for
 212 every trial. The selection of the form in Eq. (8) encapsulates wall avoidance behavior of the fish and ensures
 213 that fish remain within the boundary of the tank; this selection does not capture wall-following behavior.

214 We finally model the jump noise for the i -th fish as a compounded Poisson process,

$$J_i(t) = \sum_{k=1}^{m_i(t)} A_{k,i}(t). \quad (9)$$

215 Here, $A_{k,i}(t)$'s are independent and identically distributed Gaussian random variables with zero mean
 216 and variance γ_i^2 [$\text{rad}^2 \text{s}^{-2}$], and the total number of jumps at time t , $m_i(t)$, is such that its increments
 217 are Poisson random variables with parameter $\lambda_i(t'' - t')$ for time t', t'' and $t'' > t'$, with λ_i [s^{-1}] being
 218 frequency of jumps.

219 3.3 Model calibration

220 For each fish in the group, $i = 1, \dots, N$, we calibrated the set of locomotion and social interaction model
 221 parameters. The transition probabilities for the discrete-time Markov chain model were obtained by simply
 222 counting instances of freezing and transitions to swimming in the experimental time-series. On the other
 223 hand, maximum likelihood estimation was applied to calibrate the locomotion model parameters.

224 In summary, we calibrated the following parameters: transition probabilities, $p_{\text{FS},i}$ and $p_{\text{SF},i}$; linear
 225 expansion rate, η_i ; strength of added noise on speed, $\sigma_{v,i}$; relaxation rate, α_i ; strength of added noise
 226 on turn-rate, $\sigma_{\omega,i}$; intensity of jump turns, γ_i ; frequency of jump turns, λ_i ; alignment gains of treated to
 227 untreated fish, $k_{v_{\text{TU}}}$, untreated to treated fish, $k_{v_{\text{UT},i}}$, and between untreated fish, $k_{v_{\text{UU},i}}$; attraction gains of
 228 treated to untreated fish, $k_{p_{\text{TU}}}$, untreated to treated fish, $k_{p_{\text{UT},i}}$, and between untreated fish, $k_{p_{\text{UU},i}}$. Given
 229 that five fish comprised each of the groups, a total of 58 parameters were calibrated per trial.

230 3.3.1 Calibration of the discrete-time Markov model for freezing

231 We obtained the binary sequences $\{\Gamma_i(nT_F)\}_{n=1}^{\Upsilon}$ from the experimental time-series for each fish in
 232 the group. Similar to Burbano-Lombana and Porfiri (2020), we estimated the transition probabilities as
 233 follows:

$$p_{\text{SF},i} = \frac{N_{\text{SF},i}}{N_{\text{SS},i} + N_{\text{SF},i}}, \quad (10a)$$

$$p_{\text{FS},i} = \frac{N_{\text{FS},i}}{N_{\text{FF},i} + N_{\text{FS},i}}, \quad (10b)$$

234 where $N_{SF,i}$ and $N_{FS,i}$ are the number of transitions by the i -th fish from swimming to freezing and
 235 from freezing to swimming, respectively. $N_{SS,i}$ and $N_{FF,i}$ are the number of instances in which the fish
 236 maintained the swimming or freezing state, respectively.

237 Estimated transition probabilities for the treated fish in the group are shown in Tab. S2. For completeness,
 238 in Tab. S3, we also report a summary of the transition probabilities for the discrete-time Markov chain of
 239 the untreated fish in terms of mean and standard deviation calculated across all trials.

240 3.3.2 Calibration of the locomotion and interaction models through maximum-likelihood
 241 estimation

242 Using the experimental sampling time Δ as the time-step for discretization, we approximated Eqs. (3)
 243 and (5) using the Euler-Maruyama method as follows (Higham., 2001):

$$v_{S,i}((k+1)\Delta) = (1 + \eta_i \Delta) v_{S,i}(k\Delta) - \frac{\Delta}{\text{std}_{\omega,i} \text{BL}} |\omega_{S,i}(k\Delta)| v_{S,i}^2(k\Delta) + \sigma_{v,i} \sqrt{\Delta} v_{S,i}(k\Delta) \epsilon_{v,i}(k), \quad (11)$$

244 where $\epsilon_{v,i}(k)$ is a standard Gaussian random variable, utilized to approximate the added noise.

245 We followed the same discretization approach to approximate the JPTW in Eq. (5), leading to

$$\omega_{S,i}((k+1)\Delta) = (1 - e^{-\alpha_i \Delta}) \omega_{S,i}^*(k\Delta) + e^{-\alpha_i \Delta} \omega_{S,i}(k\Delta) + \sqrt{b_i} \epsilon_{\omega,i}^1(k) + \gamma_i \zeta_i(k) \epsilon_{\omega,i}^2(k), \quad (12a)$$

$$b_i = \frac{\sigma_{\omega,i}^2 (1 - e^{-2\alpha_i \Delta})}{2\alpha_i}, \quad (12b)$$

246 where $\epsilon_{\omega,i}^1(k)$ and $\epsilon_{\omega,i}^2(k)$ are standard Gaussian random variables and $\zeta_i(k)$ is a Bernoulli process with a
 247 probability $\Delta \lambda_i$. Wall interaction was not included in the approximation of the JPTW in Eq. (12) since we
 248 performed calibration only when the fish were more than 2 BL away from the wall.

249 For each individual, we consolidated unknown parameters in two vectors, $\varphi_{v,i}$ and $\varphi_{\omega,i}$, one for the
 250 speed and the other for the turn-rate dynamics, in Eqs. (11) and (12), respectively. These vectors were
 251 determined by solving two independent optimization problems for the speed and turn-rate. The parameters
 252 were estimated for each fish in the group independently for every trial.

253 For the approximated logistic equation in Eq. (11), the vector of unknown parameters for each fish was
 254 $\varphi_{v,i} = [\eta_i, \frac{\sigma_{v,i}}{\kappa}]^T$, where we used a scaling factor, κ , to avoid singularities at near zero swimming speed
 255 (Burbano-Lombana and Porfiri, 2020). The search was conducted within a set of admissible values χ_v
 256 selected from previous work (Mwaffo et al., 2017a). The optimization problem was solved by using as
 257 input the K_i^* samples of the speed obtained by excluding instances of freezing or swimming in proximity
 258 of the wall.

259 The maximum-likelihood estimation problem was formulated as

$$\hat{\varphi}_{v,i} = \underset{\varphi_{v,i} \in \chi_v}{\text{argmin}} - \left[\sum_{k=1}^{K_i^*} \log l_{v,i}(\varphi_{v,i}, v_{S,i}(k\Delta), \omega_{S,i}(k\Delta)) \right]. \quad (13)$$

260 The likelihood function, $l_{v,i}(\varphi_{v,i}, v_{S,i}(k\Delta), \omega_{S,i}(k\Delta))$, was derived from the model approximation in Eq.
 261 (11) as

$$l_{v,i}(\varphi_{v,i}, v_{S,i}(k\Delta), \omega_{S,i}(k\Delta)) = H \left(q_i(k\Delta), \sqrt{\sigma_{v,i}^2 \Delta} \right), \quad (14)$$

262 where $H(x, \sigma)$ is the Gaussian distribution at x with zero mean and variance σ^2 . Further, $q_i(k\Delta)$ is given
 263 by

$$q_i(k\Delta) = -\frac{1 + \eta_i}{\kappa} + \frac{\omega_{S,i}(k\Delta) v_{S,i}(k\Delta) \Delta}{\kappa \text{ BL std}_{\omega,i}} + \frac{v_{S,i}((k+1)\Delta)}{\kappa v_{S,i}(k\Delta)}. \quad (15)$$

264 Heuristically, we found that $\kappa = 5$ guarantees convergence of the optimization problem.

265 A similar approach was adopted to calibrate the discrete JPTW in Eq. (12). For each fish, we
 266 solved the optimization problem for the vector of unknown parameters for each fish, $\varphi_{\omega,i} =$
 267 $[\alpha_i, \sigma_{\omega,i}, \gamma_i, \lambda_i, k_{p_{ij}}, k_{v_{ij}}]^T$, with $j = 1, \dots, N$, $j \neq i$, where the interaction gains are categorized in
 268 accordance with Eq. (7). We used an input of K_i^* samples of the turn-rate obtained by excluding instances
 269 of freezing or swimming in proximity of the wall. In addition, the search was done within a set of admissible
 270 values χ_ω selected from Butail et al. (2016) and Mwaffo et al. (2017a). The maximum-likelihood estimation
 271 problem was formulated as

$$\hat{\varphi}_{\omega,i} = \underset{\varphi_{\omega,i} \in \chi_\omega}{\operatorname{argmin}} - \left[\sum_{k=1}^{K_i^*} \log l_{\omega,i}(\varphi_{\omega,i}, v_{S,i}(k\Delta), \omega_{S,i}(k\Delta)) \right], \quad (16)$$

272 where χ_ω is in \mathbb{R}^6 for the treated fish ($i = 1$) and χ_ω is in \mathbb{R}^8 for the untreated fish ($i \neq 1$). The likelihood
 273 function $l_{\omega,i}(\varphi_{\omega,i}, v_{S,i}(k\Delta), \omega_{S,i}(k\Delta))$ is defined as

$$l_{\omega,i}(\varphi_{\omega,i}, v_{S,i}(k\Delta), \omega_{S,i}(k\Delta)) = (1 - \lambda_i \Delta) H \left(z_i(k\Delta), \sqrt{b_i} \right) + \lambda_i \Delta H \left(z_i(k\Delta), \sqrt{(b_i + \gamma_i^2)} \right), \quad (17)$$

274 and $z_i(k\Delta)$ is

$$z_i(k\Delta) = \omega_{S,i}((k+1)\Delta) - [\omega_{S,i}(k\Delta) e^{-\alpha_i \Delta} + \omega_{S,i}^*(k\Delta) (1 - e^{-\alpha_i \Delta})]. \quad (18)$$

275 The locomotion parameters of each treated fish for all trials are displayed in Tab. S4. A summary of the
 276 parameters of the untreated fish in Tab. S5 in terms of mean and standard deviation calculated across all
 277 trials.

278 Table S6 displays the attraction gains of the treated fish $k_{p_{TU}}$, and the attraction gains of the untreated
 279 subject towards treated neighbors $\hat{k}_{p_{UT}}$ and untreated neighbors $\hat{k}_{p_{UU}}$ where a hat denotes the average of
 280 untreated individuals in each trial. Similarly, Tab. S7 contains the alignment gains of the treated fish $k_{v_{TU}}$,
 281 and the alignment gains of untreated subjects towards treated neighbors $\hat{k}_{v_{UT}}$ and untreated neighbors $\hat{k}_{v_{UU}}$.
 282 We discarded two additional trials from 25 mg/L and one additional trial from 50 mg/L due to divergence
 283 of the estimator, where interaction gains converged to their upper bounds.

284 3.3.3 Calibration of wall function

285 We relied on the work of Burbano-Lombana and Porfiri (2020) to obtain the wall function parameters in
 286 Eq. (8). The wall interaction function was calibrated for a fish swimming alone, from the data-set of Neri
 287 et al. (2019), using a wall-corrected turn-rate from the real time-series of the turn-rate of fish swimming
 288 alone,

$$\omega_c(k\Delta) = \begin{cases} |\omega_a(k\Delta)|, & \text{if } \text{sgn}(\omega_a(k\Delta)) = \text{sgn}(\phi_w(k\Delta)) \\ -|\omega_a(k\Delta)|, & \text{otherwise} \end{cases}, \quad (19)$$

289 where $\omega_a(k\Delta)$ is the turn-rate of the fish swimming alone and $\omega_c(k\Delta)$ is the corrected turn-rate. Next,
 290 $\omega_c(k\Delta)$ was plotted against the distance from the wall $d_w(k\Delta)$ where only the positive values of the
 291 corrected turn-rate were considered to capture wall avoidance. A robust non-parametric locally weighted
 292 least squares (RLOESS) function in MATLAB was used to fit the signal to a parametric exponential
 293 function. As such, the wall interaction parameters were obtained by calculating the average across all trials
 294 as $a_w = 11.68 \text{ rad s}^{-2}$ and $b_w = 0.19 \text{ cm}^{-1}$.

4 RESULTS

295 We began our analysis of the model by examining the influence of caffeine concentration on fish locomotion
 296 in terms of the variations of relevant model parameters. With respect to parameters pertaining to freezing
 297 response and locomotion, we compared with model parameters obtained in Burbano-Lombana and Porfiri
 298 (2020) to assess the effect of the social environment on fish response to caffeine administration. Finally,
 299 we conducted *in-silico* experiments to demonstrate the predictive power of the model in anticipating
 300 experimental results on schooling, and shoaling.

301 4.1 Analysis of model parameters

302 First, we investigated the effect of caffeine concentration and social environment on the locomotion
 303 parameters of the treated fish, utilizing two-way ANOVA with caffeine concentration and social
 304 environment (single or group) as independent variables. Second, we conducted ANOVA comparisons
 305 with caffeine concentration as a single independent variable to compare the interaction parameters across
 306 concentrations. Post-hoc comparisons were conducted using Tukey's HSD (honestly significant difference).
 307 The significance level was set to 0.050 throughout.

308 We found that caffeine concentration did not influence the Markov chain transition probabilities p_{FS}
 309 ($F_{3,50} = 0.424, p = 0.738$) and p_{SF} ($F_{3,50} = 0.125, p = 0.944$), neither in isolation nor in group (shown
 310 in Fig. 3A and 3B, respectively). No difference was found across social environment with respect to p_{FS}
 311 ($F_{1,50} = 0.630, p = 0.443$). Although we registered a dependence on the social environment with respect
 312 to p_{SF} ($F_{1,50} = 5.416, p = 0.027$), we did not detect any variation in post-hoc analysis. The interaction
 313 between the two independent variables was found to be not significant for both p_{FS} ($F_{3,50} = 1.733,$
 314 $p = 0.181$) and p_{SF} ($F_{3,50} = 0.812, p = 0.497$).

315 Likewise, the linear expansion rate, η , was not influenced by either caffeine concentration ($F_{3,50} = 1.264$,
316 $p = 0.297$) or social environment ($F_{1,50} = 0.698$, $p = 0.407$), shown in Fig. 4A. Further we did not
317 detect differences in the interaction of the independent variables on η ($F_{3,50} = 0.048$, $p = 0.986$). In
318 terms of the strength of added noise on the speed evolution, σ_v , we found a dependence on caffeine
319 concentration ($F_{3,50} = 3.039$, $p = 0.038$; Fig. 4B), which, however was not accompanied by variations in
320 post-hoc analysis. We found that the presence of the social environment had an effect on σ_v ($F_{1,50} = 33.21$,
321 $p < 0.001$), and post-hoc analysis indicated a decrease in the strength of added noise in the presence of
322 untreated subjects for 0 mg/L. We did not detect a significant interaction between the independent variables
323 on σ_v ($F_{3,50} = 1.088$, $p = 0.363$).

324 With respect to the turn-rate model parameters, we did not detect an effect of caffeine concentration
325 on the mean reversion rate, α ($F_{3,50} = 1.368$, $p = 0.263$). Although we found α to be affected by the
326 social environment ($F_{3,50} = 15.49$, $p < 0.001$; Fig. 5A), post-hoc analysis did not reveal significant
327 differences between concentrations. Likewise, we did not detect a significant interaction between caffeine
328 concentration and social environment on α ($F_{3,50} = 0.519$, $p = 0.672$). While caffeine concentration was
329 found to have an influence on the strength of added noise in the turn-rate evolution, σ_ω ($F_{3,50} = 2.926$,
330 $p = 0.043$; Fig. 5B), no variations were identified in post-hoc analysis. We determined a modulatory role
331 of the social environment ($F_{3,50} = 24.83$, $p < 0.001$), where σ_ω increased in the presence of a social
332 group for 50 mg/L in post-hoc analysis. No significant interaction was detected between the independent
333 variables with respect to σ_ω ($F_{3,50} = 0.866$, $p = 0.465$). With respect to intensity of jumps, γ , we found
334 caffeine concentration to play a modulatory role ($F_{3,50} = 5.760$, $p = 0.002$; Fig. 5C), with post-hoc
335 analysis revealing a decrease in the intensity of jumps for treated fish swimming in isolation from 50
336 to 70 mg/L. In addition, we found the social environment to influence γ ($F_{1,50} = 15.90$, $p < 0.001$),
337 where we detected an increase in the jump intensity in the presence of untreated subjects for 0 mg/L
338 in post-hoc analysis. We did not identify a significant interaction between caffeine concentration and
339 social environment with respect to γ ($F_{3,50} = 0.747$, $p = 0.529$). Finally, the frequency of jumps, λ , was
340 not affected by caffeine concentration ($F_{3,50} = 2.166$, $p = 0.104$). In contrast, we detected significant
341 differences across social environment ($F_{1,50} = 13.65$, $p < 0.001$; Fig. 5D). Post-hoc analysis revealed that
342 fish swimming in isolation had higher values of λ than those swimming in group for the 25 mg/L treatment.
343 We registered a significant interaction of the independent variables on λ ($F_{3,50} = 2.924$, $p = 0.048$).

344 Next, we investigated the effect of caffeine concentration on the interaction gains in the turn-rate model,
345 as shown in Fig. 6. We identified an effect of caffeine concentration on the attraction gain of the treated fish
346 towards untreated fish, $k_{p_{TU}}$ ($F_{3,22} = 3.323$, $p = 0.038$), but post-hoc analysis did not detect differences
347 between concentrations. The average attraction gain, $\hat{k}_{p_{UT}}$, of the untreated fish towards treated fish
348 was not found to vary with caffeine concentration ($F_{3,22} = 0.588$, $p = 0.629$). We determined that the
349 average attraction gain of the untreated fish towards other untreated subjects, $\hat{k}_{p_{UU}}$, varied with caffeine
350 concentration ($F_{3,22} = 3.679$, $p = 0.028$), and post-hoc analysis brought to light a decrease from 0 to
351 25 mg/L. Finally, the alignment gains were indistinguishable with respect to caffeine concentration: $k_{v_{TU}}$
352 ($F_{3,22} = 1.252$, $p = 0.315$), $\hat{k}_{v_{UT}}$ ($F_{3,22} = 0.756$, $p = 0.531$), and $\hat{k}_{v_{UU}}$ ($F_{3,22} = 0.596$, $p = 0.459$).

353 In summary, among all the freezing and locomotion parameters, we only found the intensity of jumps
354 to depend on caffeine concentration, yet, without differences with respect to vehicle-treated individuals.
355 Comparisons across social environment revealed variations in the strength of added noise on both speed and
356 turn-rate and in the jump parameters. Swimming in group reduced the strength of the added noise on the
357 speed evolution of vehicle-treated subjects, and it increased the strength of the added noise on the turn-rate
358 evolution at the intermediate concentration. Further, while the presence of a social group increased the

359 intensity of jumps of vehicle-treated subjects, it reduced the frequency of jumps of individuals treated at a
 360 low concentration. Parameters pertaining to social response were generally robust with respect to caffeine
 361 concentration, except for the attraction of untreated fish towards other untreated subjects, with low caffeine
 362 concentration causing a reduction in alignment.

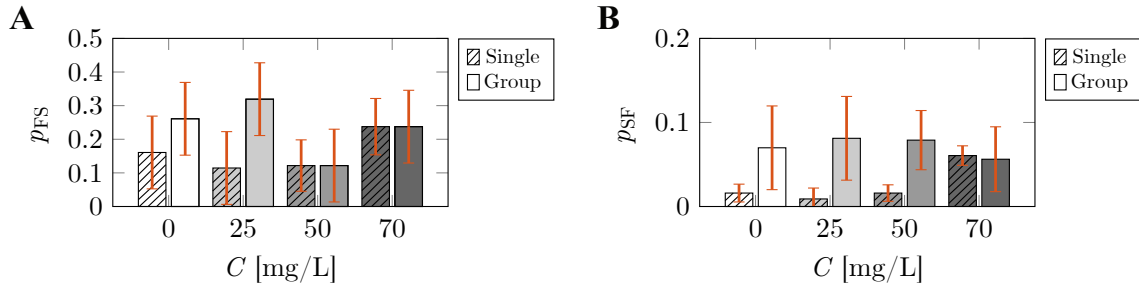


Figure 3. Comparisons of discrete-time Markov chain parameters of the treated fish across caffeine concentrations and social environment (single or group). The bars represent the mean value of the probability of transition from freezing to swimming (A), and the mean value of the probability of transition from swimming to freezing (B). The striped bars correspond to the calibrated parameters for the case of a single treated fish from Burbano-Lombana and Porfiri (2020). The solid bars correspond to the calibrated parameters for the case of a treated fish swimming in a social group. The vertical red error bars represent standard errors of the means.

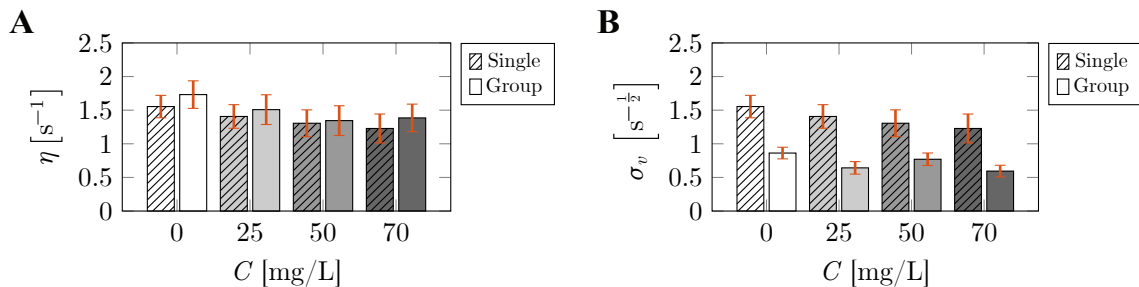


Figure 4. Comparisons of the locomotion parameters corresponding to the speed evolution of the treated fish across caffeine concentrations and social environment (single or group). The bars represent the mean value of the linear expansion rate (A), and strength of added noise in the speed evolution (B). The striped bars correspond to the calibrated parameters for the case of a single treated fish from Burbano-Lombana and Porfiri (2020). The solid bars correspond to the calibrated parameters for the case of a treated fish swimming in a social group. The symbol \$ indicates a significant difference ($p < 0.050$) in Tukey's HSD post-hoc analysis comparing individuals swimming alone or on group (single versus group). The vertical red error bars represent standard errors of the means.

363 4.2 *In-silico* experiments

364 We conducted *in-silico* experiments to validate the developed model and investigate its ability to predict
 365 the social behavior of fish detected from experimental time-series (Neri et al., 2019), for a range of
 366 interaction metrics that quantify schooling, and shoaling.

367 Schooling is a measure of fish tendency to align their bodies during swimming (Pitcher et al., 1986;
 368 Miller and Gerlai, 2012). The degree of alignment among the four untreated fish was scored in terms of the
 369 instantaneous polarization (Aureli et al., 2012),

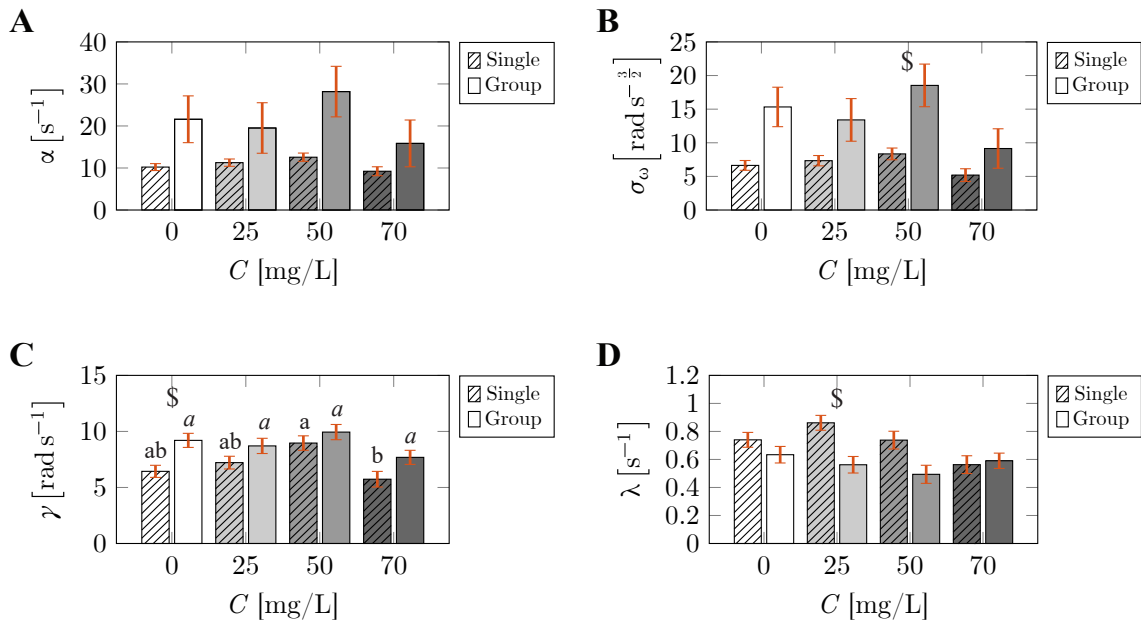


Figure 5. Comparisons of the locomotion parameters corresponding to the turn-rate evolution of the treated fish across caffeine concentrations, and social environment (single or group). The bars represent the mean value of the mean reversion rate (**A**), strength of added noise in the turn-rate evolution (**B**), intensity of jumps in the turn-rate evolution (**C**), and frequency of jumps in turn-rate evolution (**D**). The striped bars correspond to the calibrated parameters for the case of a single treated fish from Burbano-Lombana and Porfiri (2020). The solid bars correspond to the calibrated parameters for the case of a treated fish swimming in a social group. Different letters on top of the bars indicate a significant difference ($p < 0.050$) in Tukey's HSD post-hoc analysis across caffeine concentrations, comparing individuals swimming in isolation (standard font) or in group (Italic font). The symbol $\$$ indicates a significant difference ($p < 0.050$) in Tukey's HSD post-hoc analysis comparing individuals swimming alone or on group (single versus group). The vertical red error bars represent standard errors of the means.

$$P(k\Delta) = \frac{1}{N-1} \left\| \sum_{i=2}^N \frac{\mathbf{v}_i(k\Delta)}{v_i(k\Delta)} \right\|, \quad (20)$$

370 where $N = 5$ is the number of fish in the experiment. Polarization varies between 0 and 1, where 1
 371 identifies the case in which untreated fish are perfectly aligned in the same direction.

372 The alignment between the treated fish and the untreated group of fish was scored in terms of the relative
 373 instantaneous polarization, $R(k\Delta)$,

$$R(k\Delta) = \frac{\mathbf{v}_1(k\Delta)^T}{v_1(k\Delta)} \frac{1}{N-1} \sum_{i=2}^N \frac{\mathbf{v}_i(k\Delta)}{v_i(k\Delta)}, \quad (21)$$

374 Relative polarization ranges between -1 and 1 , where 1 corresponds to the group of untreated fish pointing
 375 in the same direction of the treated fish, and -1 indicates that the treated fish is pointing in the opposite
 376 direction to the group of untreated fish. These quantities were averaged in time to compute the average
 377 polarization and the average relative polarization.

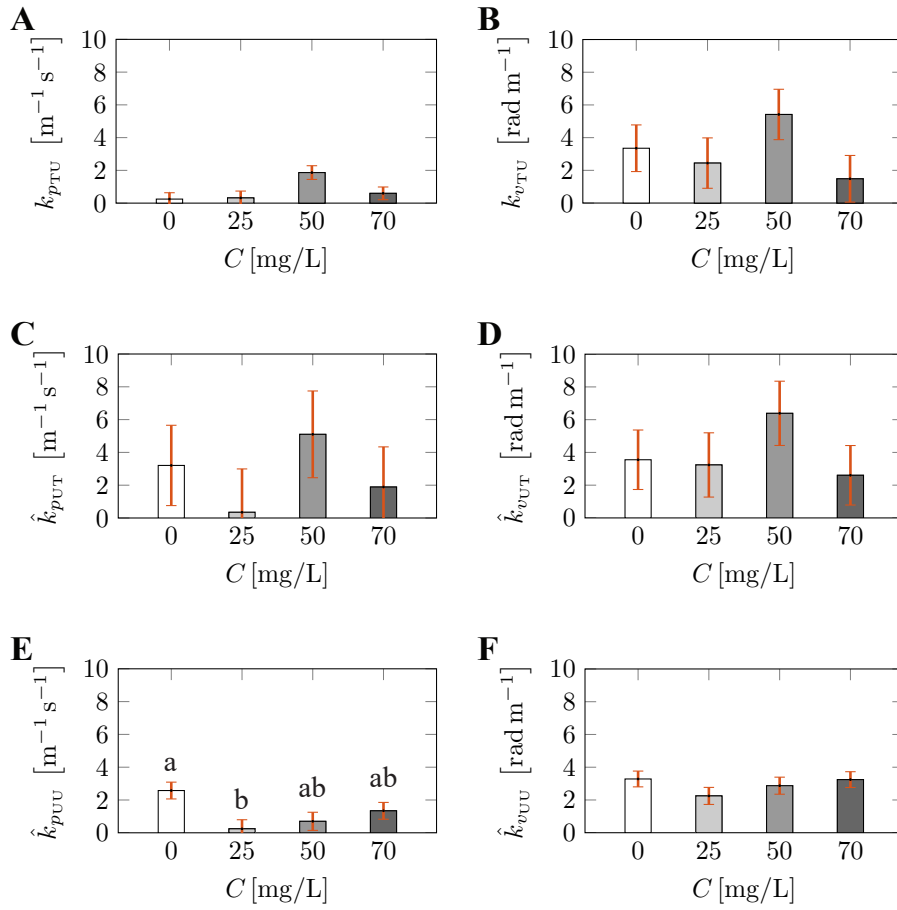


Figure 6. Calibrated interaction parameters in the turn-rate evolution across caffeine concentrations. The bars represent the mean value of the attraction gain of treated fish towards untreated fish (**A**), alignment gain of treated fish towards untreated fish (**B**), average attraction gain of untreated fish towards treated fish (**C**), average alignment gain of untreated fish towards treated fish (**D**), average attraction gain between untreated fish (**E**), and average alignment gain between untreated fish (**F**). Different letters on top of the bars indicate a significant difference ($p < 0.050$) in Tukey's HSD post-hoc analysis across caffeine concentrations. The vertical red error bars represent standard errors of the means.

378 To quantify fish shoaling, the tendency of fish to swim in close proximity, we computed the inter-
 379 individual distance, $d_{ij}(k\Delta)$, between each pair in the group. We scored the average distance between the
 380 treated and untreated subjects, and the average distance among untreated individuals.

381 We conducted *in-silico* experiments using the model parameters for the case of in-group swimming,
 382 shown in solid bars in Fig. 3-6. Ten simulations were performed for each of the four caffeine concentrations.
 383 For each fish in all 40 trials, the interaction gains were sampled from a Gaussian distribution with mean
 384 and standard deviation of the corresponding parameter at that concentration. On the other hand, since we
 385 did not find any effect of caffeine concentration on the transition probabilities and locomotion parameters
 386 for in-group swimming, those parameters were taken as the average of all fish across all experimental trials
 387 based on treatment. The initial conditions $x_i(0)$, $y_i(0)$, $\theta_i(0)$, $\Gamma_i(0)$, $v_i(0)$, and $\omega_i(0)$ were chosen uniformly
 388 at random in their respective intervals. Time-series of four trajectories for each caffeine concentration are
 389 shown in Fig. 7; videos are presented in the supplemental material. Note that the wall function adopted in

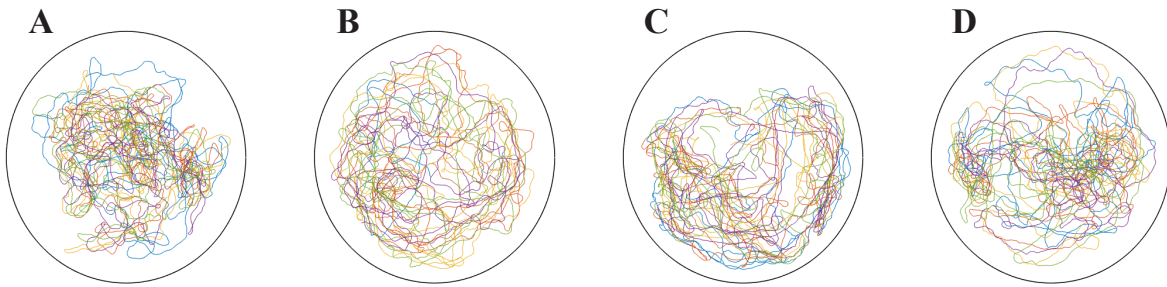


Figure 7. Representative *in-silico* trajectories of a group of five subjects, with four untreated individuals and one subjects treated at a caffeine concentration of: 0 (**A**), 25 (**B**), 50 (**C**), and 70 mg/L (**D**).

390 this study does not take into consideration the wall following behavior of zebrafish, thus explaining the
 391 differences in wall interactions between *in-silico* trajectories in Fig. 7 and experimental ones in Fig. 1.

392 We performed statistical analysis to compare the social interaction metrics across caffeine concentrations,
 393 and validate the *in-silico* results against those obtained from real experiments. For this purpose, we
 394 conducted two-way ANOVA with caffeine concentration and data-type (experiments or *in-silico*) as
 395 independent variables. Post-hoc comparisons were conducted using Tukey's HSD. The significance level
 396 was set to 0.050 throughout.

397 We detected influence of caffeine concentration on the average polarization, \bar{P} ($F_{3,61} = 7.781, p <$
 398 0.001), shown in Fig. 8A. Post-hoc analysis revealed differences in experimental results, where the average
 399 polarization was found to increase from 0 to 50 mg/L. Comparisons across data-types did not indicate
 400 differences between real and *in-silico* experiments ($F_{3,61} = 1.354, p = 0.249$). Likewise, no interaction
 401 between the independent variables was identified on \bar{P} ($F_{3,61} = 0.675, p = 0.571$). With respect to
 402 the average relative polarization, \bar{R} (Fig. 8B), we did not find an effect on either caffeine concentration
 403 ($F_{3,61} = 1.354, p = 0.071$) or data-type ($F_{1,61} = 0.229, p = 0.634$), although we identified significant
 404 interaction ($F_{3,61} = 3.855, p = 0.014$).

405 Next, we found that the shoaling tendency between the treated fish and untreated subjects, in terms of
 406 the average distance \bar{d}_{T-U} , was consistent across caffeine concentrations ($F_{1,61} = 1.849, p = 0.179$) and
 407 data-types ($F_{1,61} = 1.461, p = 0.234$), as shown in Fig. 9A. No interaction was detected between the
 408 independent variables on \bar{d}_{T-U} ($F_{3,61} = 0.262, p = 0.853$). In contrast, we detected an effect of caffeine
 409 concentration on the average distance between the untreated fish, \bar{d}_{U-U} ($F_{3,61} = 12.16, p < 0.001$;
 410 Fig. 9B). Post-hoc analysis revealed a decrease in \bar{d}_{U-U} from 25 to 50 mg/L in the experimental data-
 411 set. Similar differences were found in the *in-silico* data-set where \bar{d}_{U-U} was larger for 25 mg/L than 0
 412 and 50 mg/L. While comparisons between data-types revealed a significant difference ($F_{1,61} = 11.29,$
 413 $p = 0.0001$), the results were indistinguishable between real and *in-silico* experiments in post-hoc
 414 analysis. Finally, we did not detect a significant interaction between the independent variables on \bar{d}_{U-U}
 415 ($F_{3,61} = 2.354, p = 0.081$).

5 DISCUSSION

416 In this work, we developed a modeling framework to study the effect of acute caffeine treatment on the
 417 social behavior of zebrafish. We contributed two key advances to previous work on modeling collective
 418 behavior of zebrafish. First, similar to the analysis with respect to zebrafish swimming alone in Burbano-
 419 Lombana and Porfiri (2020), we included the freezing response of each individual within the group, which

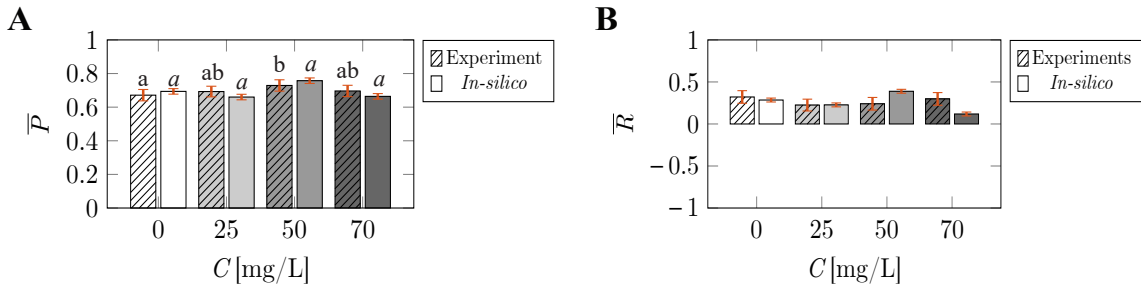


Figure 8. Comparisons of the schooling tendency of the fish, measured in terms of average polarization (A), and average relative polarization (B), across caffeine concentrations and data-types (experiment or *in-silico*). Different letters on top of the bars indicate a significant difference ($p < 0.050$) in Tukey's HSD post-hoc analysis across caffeine concentrations, comparing interaction metrics in experiment (standard font) or *in-silico* (Italic font) data-type. The vertical red error bars represent standard errors of the means.

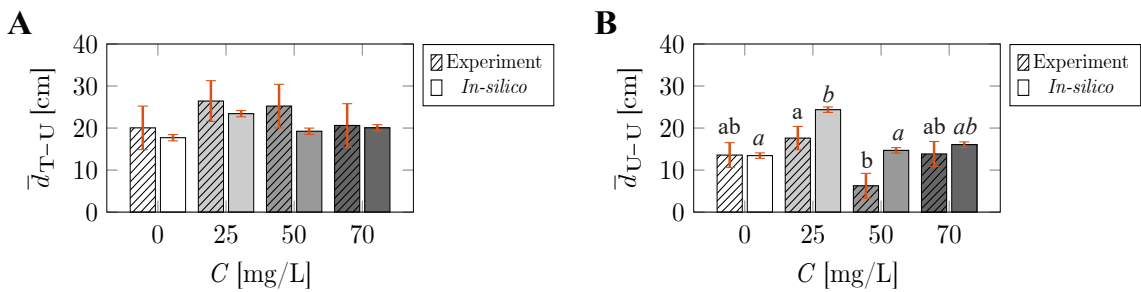


Figure 9. Comparisons of the shoaling tendency of the fish, measured in terms of the average distance between treated fish and untreated fish (A), and average distance between untreated fish (B), across caffeine concentrations and data-types (experiment or *in-silico*). Different letters on top of the bars indicate a significant difference ($p < 0.050$) in Tukey's HSD post-hoc analysis across caffeine concentrations, comparing interaction metrics in experiment (standard font) or *in-silico* (Italic font) data-type. The vertical red error bars represent standard errors of the means.

420 is necessary to capture anxiety-related behavior in response to caffeine (Maximino et al., 2011). For this
 421 purpose, we developed a two-time-scale modeling dichotomy. Along a slow time-scale, we used a discrete-
 422 time Markov chain to describe the transition between swimming and freezing states. At a fast time-scale,
 423 we modeled the evolution of the speed and turn-rate during swimming as a system of coupled SDEs: a
 424 logistic equation to represent the speed and a JPTW to describe the turn-rate. Second, we granularly tracked
 425 the directional interaction between each pair of fish based on the treatment of each fish within the pair. This
 426 approach takes into consideration previous experimental work highlighting the effect of caffeine on the
 427 behavioral response of treated fish and its appraisal by untreated conspecifics (Gupta et al., 2014; Miller
 428 and Gerlai, 2007).

429 We calibrated the model on real experimental data from previous work (Neri et al., 2019), where we
 430 studied groups of caffeine-treated subject and untreated individuals swimming in a shallow water tank.
 431 For each group of five individuals, we estimated 20 parameters, entering the Markov chain and the SDEs.
 432 Calibration employed a combination of maximum likelihood estimation and classical plug-in estimation.
 433 We display our results on two fronts. First, we compared the model parameters obtained for a treated fish
 434 swimming with untreated subjects with those obtained by Burbano-Lombana and Porfiri (2020) for the case
 435 of an isolated fish. Second, we compared the social interaction metrics, in terms of average polarization,

436 average relative polarization, and average inter-individual distance, between the experimental and *in-silico*
437 data-sets.

438 In contrast with our expectations, we did not observe a modulatory role of caffeine on freezing and
439 locomotion parameters. Our expectation was based on a number of previous studies documenting a robust
440 dependence of zebrafish behavioral response to acute caffeine administration (Maximino et al., 2010a;
441 Stewart et al., 2010). This was particularly evident for individuals swimming with untreated subjects, for
442 which we failed to detect any effect of caffeine treatment. Likely, the explanation for the abolishment of a
443 dose-dependent response should be sought in the presence of the social environment, which, indeed was
444 responsible for a few, salient variations in locomotion parameters associated with the speed and turn-rate
445 evolution. It is tenable that the presence of social cues had a leveling role on the anxiogenic effect of
446 caffeine, which is indirectly evidenced by the tendency to enhance white noise with respect to the jump
447 noise in the turn-rate evolution. Jumps have been associated with erratic activity of the animal, in the
448 form of C- and U-turns, so that their reduction in favor of steady swimming offers an indication of an
449 anxiolytic value of the social environment, also discussed by Neri et al. (2019). With respect to the effect on
450 untreated subjects, we recorded a decrease in their tendency to shoal with each other, which highlights
451 an interesting, albeit indirect, effect of caffeine treatment. Caffeine treatment of one selected individuals
452 might bear an anxiolytic effect on the rest of the group that reduce their tendency to stay close (Miller and
453 Gerlai, 2007; Speedie and Gerlai, 2008); understanding this counter-intuitive finding should be the object
454 of future research.

455 The calibrated model is in good agreement with experimental observations on social metrics, related
456 to shoaling and schooling. While this agreement should be desired in any calibrated model, it is not
457 obvious to attain. In fact, *in-silico* experiments do not contain the fine-grain variations that are unique to the
458 experimental subjects, whereby we excluded from the simulations any statistical variation in the locomotion
459 and freezing parameters. Accounting for variations in the social gains due to caffeine administration through
460 a simple normal distribution seems sufficient to capture the emergent response of the groups, as well as the
461 role of the treated individual.

462 The proposed model is not free of limitations. First, we assumed that the interaction between fish is solely
463 based on visual stimuli. Incorporating other mechanisms of social interactions, such as hydro interactions
464 (Gazzola et al., 2016; Porfiri et al., to appear), may help refine the mathematical model, especially in
465 terms of short-range interactions related to the perturbations they create in the fluid environment (Porfiri
466 et al., to appear). Second, the current model does not incorporate wall following behavior observed in
467 real experiments, whereby interaction with the wall is limited to a simple repulsion (Gautrais et al., 2009).
468 Third, the model is purely two-dimensional, thereby failing to capture salient anxiety-related responses that
469 have been documented in zebrafish, such geotaxis (Maximino et al., 2010a,b). Fourth, the entire modeling
470 framework is based on a single psychoactive compound, which bears limitations in the generalizations of
471 the predictions to other substances that impinge on anxiety (da Silva Chaves et al., 2018; Kacprzak et al.,
472 2017). Along this line, the most fundamental limitations of the model is the lack of a direct link between
473 the molecular composition of the substance or the brain mechanisms it affects and the parameters of the
474 model. In its present incarnation, the model requires knowledge of all the model parameters to perform
475 *in-silico* experiments, without allowing for exploring different substances or even untested concentrations
476 on caffeine.

477 Despite these limitations, the proposed model offers a first step in the design of *in-silico* experiments that
478 can aid the 3R's with respect to zebrafish experimentation. The proposed model can be used to reduce the
479 number of experiments, by affording statistical insight into the sample size. Likewise, the model can be

480 used to refine existing data-sets, by informing model-based analysis of the data and, potentially, assist in
481 verification and tracking. Finally, pilot studies could be conducted on a computer, thereby reducing the
482 number of subjects utilized in experimental research.

CONFLICT OF INTEREST STATEMENT

483 The authors declare that the research was conducted in the absence of any commercial or financial
484 relationships that could be construed as a potential conflict of interest.

AUTHOR CONTRIBUTIONS

485 MP designed and supervised the research. MT developed the computer codes, conducted model calibration,
486 performed statistical analysis, and wrote a first, preliminary draft of the work. MP consolidated the draft in
487 the present submission. Both authors developed the mathematical model and analyzed results.

FUNDING

488 This work was supported by National Science Foundation under grant number CMMI 1901697, and the
489 National Institutes of Health, National Institute on Drug Abuse under grant number 1R21DA042558-01A1
490 and the Office of Behavioral and Social Sciences Research that co-funded the National Institute on Drug
491 Abuse grant, all awarded to MP. The funders had no role in study design, data collection and analysis,
492 decision to publish, or preparation of the manuscript.

SUPPLEMENTAL DATA

493 The supplemental data include a list of notation and variables used throughout the paper. In addition,
494 calibrated parameters for the treated fish from each trial and summaries of the locomotion parameters of
495 the untreated fish across all trials, are displayed in tables.

DATA AVAILABILITY STATEMENT

496 The experimental data-set and representative videos of the *in-silico* experiments can be found in the
497 repository of our research laboratory at <https://github.com/dynamicalsystemslaboratory/CaffeineSocialBehavior>

REFERENCES

499 Aureli, M., Fiorilli, F., and Porfiri, M. (2012). Portraits of self-organization in fish schools interacting with
500 robots. *Physica D: Nonlinear Phenomena* 241(9), 908–920

501 Badyal, D. and Desai, C. (2014). Animal use in pharmacology education and research: The changing
502 scenario. *Indian Journal of Pharmacology* 46(3), 257–265

503 Berdahl, A., Torney, C. J., Ioannou, C. C., Faria, J. J., and Couzin, I. D. (2013). Emergent sensing of
504 complex environments by mobile animal groups. *Science* 339(6119), 574–576

505 Blake, R. W. (2004). Fish functional design and swimming performance. *Journal of Fish Biology* 65(5),
506 1193–1222

507 Burbano-Lombana, D. A. and Porfiri, M. (2020). Data-driven modeling of zebrafish behavioral response to
508 acute caffeine administration. *Journal of Theoretical Biology* 485, 11054

509 Butail, S., Mwaffo, V., and Porfiri, M. (2016). Model-free information-theoretic approach to infer
510 leadership in pairs of zebrafish. *Physical Review E* 93(4), 042411

511 Cachat, J., Canavello, P., Elegante, M., Bartels, B., Hart, P., Bergner, C., et al. (2010). Modeling withdrawal
512 syndrome in zebrafish. *Behavioural Brain Research* 208(2), 371 – 376

513 Calovi, D., Litchinko, A., Lecheval, V., Lopez, U., Escudero, A., Chaté, H., et al. (2018). Disentangling
514 and modeling interactions in fish with burst-and-coast swimming reveal distinct alignment and attraction
515 behaviors. *PLoS Computational Biology* 14(1), e1005933

516 Calovi, D. S., Lopez, U., Schuhmacher, P., Chaté, H., Sire, C., and Theraulaz, G. (2015). Collective
517 response to perturbations in a data-driven fish school model. *Journal of The Royal Society Interface*
518 12(104), 20141362

519 Chow, P. K. H., Ng, R. T. H., and Ogden, B. E. (2008). *Using Animal Models in Biomedical Research*
520 (World Scientific)

521 Chung, M.-H. (2009). On burst-and-coast swimming performance in fish-like locomotion. *Bioinspiration*
522 & *Biomimetics* 4(3), 036001

523 Collignon, B., Séguert, A., and Halloy, J. (2016). A stochastic vision-based model inspired by zebrafish
524 collective behaviour in heterogeneous environments. *Royal Society Open Science* 3(1), 150473

525 da Silva Chaves, S. N., Felício, G. R., Costa, B. P. D., de Oliveira, W. E. A., Lima-Maximino, M. G.,
526 de Siqueira Silva, D. H., et al. (2018). Behavioral and biochemical effects of ethanol withdrawal in
527 zebrafish. *Pharmacology Biochemistry and Behavior* 169, 48 – 58

528 Egan, R., Bergner, C., Hart, P., Cachat, J., Canavello, P., Elegante, M., et al. (2009). Understanding
529 behavioral and physiological phenotypes of stress and anxiety in zebrafish. *Behavioural Brain Research*
530 205(1), 38–44

531 Filella, A., Nadal, F., Sire, C., Kanso, E., and Eloy, C. (2018). Model of collective fish behavior with
532 hydrodynamic interactions. *Physical Review Letters* 120, 198101

533 Ford, K. (2016). Refinement, reduction, and replacement of animal toxicity tests by computational methods.
534 *ILAR Journal* 57(2), 226–233

535 Gautrais, J., Ginelli, F., Fournier, R., Blanco, S., Soria, M., Chaté, H., et al. (2012). Deciphering interactions
536 in moving animal groups. *PLoS Computational Biology* 8(9), e1002678

537 Gautrais, J., Jost, C., Soria, M., Campo, A., Motsch, S., Fournier, R., et al. (2009). Analysis of fish
538 movement as a persistent turning walker. *Journal of Mathematical Biology* 58, 429–445

539 Gazzola, M., Tchieu, A., Alexeev, D., de Brauer, A., and Koumoutsakos, P. (2016). Learning to school in
540 the presence of hydrodynamic interactions. *Journal of Fluid Mechanics* 789, 726–749

541 Gerlai, R., Ahmad, F., and Prajapati, S. (2008). Differences in acute alcohol-induced behavioral responses
542 among zebrafish populations. *Alcoholism: Clinical and Experimental Research* 32(10), 1763–1773

543 Goldsmith, P. (2004). Zebrafish as a pharmacological tool: the how, why and when. *Current Opinion in
544 Pharmacology* 4(5), 504–512

545 Guo, S. (2004). Linking genes to brain, behavior and neurological diseases: what can we learn from
546 zebrafish? *Genes, Brain and Behavior* 3(2), 63–74

547 Gupta, P., Khobragade, S., Shingatgeri, V. M., and Rajaram, S. M. (2014). Assessment of locomotion
548 behavior in adult zebrafish after acute exposure to different pharmacological reference compounds. *Drug
549 Development and Therapeutics* 5(2), 127–133

550 Herbert-Read, J. E., Krause, S., Morrell, L. J., Schaerf, T. M., Krause, J., and Ward, A. J. W. (2013). The
551 role of individuality in collective group movement. *Proceedings of the Royal Society B: Biological
552 Sciences* 280(1752), 20122564

553 Herbert-Read, J. E., Perna, A., Mann, R. P., Schaerf, T. M., Sumpter, D. J. T., and Ward, A. J. W. (2011).
554 Inferring the rules of interaction of shoaling fish. *Proceedings of the National Academy of Sciences*
555 108(46), 18726–18731

556 Higham., D. J. (2001). An algorithmic introduction to numerical simulation of stochastic differential
557 equations. *SIAM Review* 43(3), 525–546

558 Jhawar, J., Morris, R. G., Amith-Kumar, U. R., Danny Raj, M., Rogers, T., Rajendran, H., et al. (2020).
559 Noise-induced schooling of fish. *Nature Physics* 16(4), 488–493

560 Kacprzak, V., Patel, N. A., Riley, E., Yu, L., Yeh, J.-R. J., and Zhdanova, I. V. (2017). Dopaminergic
561 control of anxiety in young and aged zebrafish. *Pharmacology Biochemistry and Behavior* 157, 1 – 8

562 Katz, Y., Tunstrøm, K., Ioannou, C. C., Huepe, C., and Couzin, I. D. (2011). Inferring the structure and
563 dynamics of interactions in schooling fish. *Proceedings of the National Academy of Sciences* 108(46),
564 18720–18725

565 Khan, K., Collier, A., Meshalkina, D., Kysil, E., Khatsko, S., Kolesnikova, T., et al. (2017).
566 Zebrafish models in neuropsychopharmacology and CNS drug discovery: Zebrafish models in
567 neuropsychopharmacology. *British Journal of Pharmacology* 174(13), 1925–1944

568 Kopman, V., Laut, J., Polverino, G., and Porfiri, M. (2013). Closed-loop control of zebrafish response using
569 a bioinspired robotic-fish in a preference test. *Journal of the Royal Society Interface* 10(78), 20120540

570 Krause, J., Ward, A. J. W., Jackson, A. L., Ruxton, G. D., James, R., and Currie, S. (2005). The influence
571 of differential swimming speeds on composition of multi-species fish shoals. *Journal of Fish Biology*
572 67(3), 866–872

573 Ladu, F., Butail, S., Macri, S., and Porfiri, M. (2014). Sociality modulates the effects of ethanol in zebra
574 fish. *Alcoholism: Clinical and Experimental Research* 38(7), 2096–2104

575 Maximino, C., da Silva, A. W., Gouveia Jr, A., and Herculano, A. M. (2011). Pharmacological analysis of
576 zebrafish (*Danio rerio*) scototaxis. *Progress in Neuro-Psychopharmacology and Biological Psychiatry*
577 35(2), 624–631

578 Maximino, C., de Brito, T., da Silva Batista, A., Herculano, A., Morato, S., and Gouveia Jr, A. (2010a).
579 Measuring anxiety in zebrafish: A critical review. *Behavioural Brain Research* 214(2), 157–171

580 Maximino, C., de Brito, T., de Mattos Dias, C., Gouveia Jr, A., and Morato, S. (2010b). Scototaxis as
581 anxiety-like behavior in fish. *Nature Protocols* 5(2), 209–216

582 Miller, N. and Gerlai, R. (2007). Quantification of shoaling behaviour in zebrafish (*Danio rerio*).
583 *Behavioural Brain Research* 184(2), 157 – 166

584 Miller, N. and Gerlai, R. (2012). From schooling to shoaling: Patterns of collective motion in zebrafish
585 (*Danio rerio*). *PLoS ONE* 7(11), e48865

586 Mwaffo, V., Anderson, R. P., Butail, S., and Porfiri, M. (2015). A jump persistent turning walker to model
587 zebrafish locomotion. *Journal of The Royal Society Interface* 12(102), 20140884

588 Mwaffo, V., Butail, S., and Porfiri, M. (2017a). *In-silico* experiments of zebrafish behaviour: Modeling
589 swimming in three dimensions. *Scientific Reports* 7, 39877

590 Mwaffo, V., Korneyeva, V., and Porfiri, M. (2017b). simUfish: An interactive application to teach K-12
591 students about zebrafish behavior. *Zebrafish* 14(5), 477–488

592 Mwaffo, V. and Porfiri, M. (2015). Turning rate dynamics of zebrafish exposed to ethanol. *International
593 Journal of Bifurcation and Chaos* 25(7), 1540006

594 Neri, D., Ruberto, T., Mwaffo, V., Bartolini, T., and Porfiri, M. (2019). Social environment modulates
595 anxiogenic effects of caffeine in zebrafish. *Behavioral Pharmacology* 30(1), 45–58

596 Pasquali, S. (2001). The stochastic logistic equation: stationary solutions and their stability. *Rendiconti del
597 Seminario Matematico della Università di Padova* 106, 165–183

598 Pitcher, T., Magurran, A., and Allan, J. (1986). Size-segregative behaviour in minnow shoals. *Journal of
599 Fish Biology* 29, 83–95

600 Porfiri, M., Karakaya, M., Sattanapalle, R. R., and Peterson, S. D. (to appear). Emergence of in-line
601 swimming patterns in zebrafish pairs. *Flow*

602 Raunio, H. (2011). *In Silico* toxicology – non-testing methods. *Frontiers in Pharmacology* 2, 33

603 Ruberto, T., Mwaffo, V., Singh, S., Neri, D., and Porfiri, M. (2016). Zebrafish response to a robotic replica
604 in three dimensions. *Royal Society Open Science* 3(10), 160505

605 Sánchez Morgado, J. M. and Brønstad, A. (2021). *Experimental Design and Reproducibility in Preclinical
606 Animal Studies* (Springer International Publishing)

607 Shirazi, M. J. and Abaid, N. (2018). Collective behavior in groups of self-propelled particles with active
608 and passive sensing inspired by animal echolocation. *Physical Review E* 98(4), 042404

609 Speedie, N. and Gerlai, R. (2008). Alarm substance induced behavioral responses in zebrafish (*Danio
610 rerio*). *Behavioral Brain Research* 188(1), 168–177

611 Stewart, A., Gaikwad, S., Kyzar, E., Green, J., Roth, A., and Kalueff, A. (2012). Modeling anxiety using
612 adult zebrafish: A conceptual review. *Neuropharmacology* 62(1), 135–143

613 Stewart, A., Kadri, F., DiLeo, J., Min Chung, K., Cachat, J., Goodspeed, J., et al. (2010). The developing
614 utility of zebrafish in modeling neurobehavioral disorders. *International Journal of Comparative
615 Psychology* 23(1), 104–120

616 Stewart, A. M., Braubach, O., Spitsbergen, J., Gerlai, R., and Kalueff, A. V. (2014). Zebrafish models for
617 translational neuroscience research: from tank to bedside. *Trends in Neurosciences* 37(5), 264–278

618 Valentini, G., Mizumoto, N., Pratt, S. C., Pavlic, T. P., and Walker, S. I. (2020). Revealing the structure of
619 information flows discriminates similar animal social behaviors. *eLife* 9, e55395

620 Viceconti, M., Pappalardo, F., Rodriguez, B., Horner, M., Bischoff, J., and Musuamba Tshinanu, F. (2021).
621 *In silico* trials: Verification, validation and uncertainty quantification of predictive models used in the
622 regulatory evaluation of biomedical products. *Methods* 185, 120–127

623 Zienkiewicz, A., Barton, D. A., Porfiri, M., and Di Bernardo, M. (2015). Data-driven stochastic modelling
624 of zebrafish locomotion. *Journal of Mathematical Biology* 71, 1081–1105

625 Zienkiewicz, A. K., Ladu, F., Barton, D. A., and Porfiri, M. (2018). Data-driven modelling of social forces
626 and collective behaviour in zebrafish. *Journal of Theoretical Biology* 443, 39–51